

# Flexible nano-GFO/PVDF piezoelectric-polymer nano-composite films for mechanical energy harvesting

Monali Mishra<sup>1,3</sup>, Amritendu Roy<sup>2</sup>, Sukalyan Dash<sup>3</sup>, Somdutta Mukherjee<sup>1</sup>

<sup>1</sup>Colloids and Materials Chemistry Department, CSIR-IMMT Bhubaneswar-751013, India

<sup>2</sup>School of Minerals, Metallurgical and Materials Engineering, Indian Institute of Technology Bhubaneswar, Bhubaneswar-752050, India

<sup>3</sup>Department of Chemistry, VSSUT Burla, Burla-768018, India

Email: [msomdutta@gmail.com](mailto:msomdutta@gmail.com)

**Abstract:** Owing to the persistent quest of renewable energy technology, piezoelectric energy harvesters are gathering considerable research interest due to their potential in driving microelectronic devices with small power requirement. Electrical energy (milli to microwatt range) is generated from mechanical counterparts such as vibrations of machines, human motion, flowing water etc. based on the principles of piezoelectricity. Flexible high piezoelectric constant ( $d_{33}$ ) ceramic/polymer composites are crucial components for fabricating these energy harvesters. The polymer composites composed of gallium ferrite nanoparticles and polyvinylidene fluoride (PVDF) as the matrix have been synthesized by solvent casting method. First, 8 wt. % PVDF was dissolved in DMF and then different compositions of GaFeO<sub>3</sub> or GFO (10, 20, 30 wt. %) (with respect to PVDF only) nanocomposites were synthesized. The phase of the synthesized nanocomposites were studied by X-Ray diffraction which shows that with the increase in the GFO concentration, the intensity of diffraction peaks of PVDF steadily decreased and GFO peaks became increasingly sharp. As the concentration of GFO increases in the PVDF polymer matrix, band gap is also increased albeit to a small extent. The maximum measured output voltage and current during mechanical pressing and releasing conditions were found to be ~ 3.5 volt and 4 nA, respectively in 30 wt % GFO-PVDF composite, comparable to the available literature.

## 1. Introduction:

In recent days the dimension and power consumption of electronic devices have reduced significantly to make them portable and convenient to use in daily requirements. Piezoelectricity based energy harvesters that convert mechanical energy to electrical energy are perfect for powering those electronic devices where various mechanical vibrations originating from human movement or movement of any machine can be utilized. This can crumb the present dependency on batteries, give more freedom to mobile consumers and minimize the environmental issue related to battery disposal.

Piezoelectric materials with large piezoelectric constants ( $d_{33}$ ) are natural choices for making composites. For this purpose various piezoelectric ceramics viz. ~ barium titanate (BaTiO<sub>3</sub>), Lead zirconium titanate (PZT), zinc oxide (ZnO), lead magnesium niobate – lead titanate (PMN-PT) have been used for their large  $d_{33}$  value. However, application prospect of these piezoelectric ceramics are limited due to their poor mechanical property, *i.e.*, brittleness. Further, piezoceramics experience fatigue crack when exposed to cyclic loading. Such unfavourable mechanical characteristics inspires the search for alternative materials with superior properties.



Polyvinylidene difluoride (PVDF) is a piezoelectric polymer which is highly flexible. PVDF thus has attracted significant research attention due to its favourable mechanical property and ferroelectric, pyroelectric and piezoelectric properties. It has a piezoelectric coefficient of 12-23 pC/N.[1] A series of studies have been performed investigating the piezoelectric based energy harvesting behaviour of PVDF. Though, the pure PVDF based devices showed generation of current in a few hundred of nAmp range the voltage generated was restricted to ~ 0.5 V resulting in a very low power output.[2, 3] In this context, piezoelectric ceramics are blended with the PVDF polymer matrix to improve output current and voltage characteristics. In the present study we have chosen gallium ferrite, GaFeO<sub>3</sub> or GFO nanopowder, a piezoelectric material with piezoelectric coefficient ~ 4 pC/N with appreciable conductivity. [4]

## 2. Experimental details:

### 2.1 Synthesis of Gallium Ferrite or GFO nanopowders:

GFO nanopowders, were synthesized using modified Pechini method.[5] gallium nitrate hydrate (Ga(NO<sub>3</sub>)<sub>3</sub> .xH<sub>2</sub>O) (sigma Aldrich ≥ 99.9%) and iron nitrate nonahydrate (Fe(NO<sub>3</sub>)<sub>3</sub>.9H<sub>2</sub>O) (sigma Aldrich ≥ 98%) were taken as the precursor materials.

### 2.2 Synthesis of GFO-PVDF nano-composites:

GFO/PVDF nano-composite was synthesized by solvent casting method. For the preparation of composites, we used N, N-Dimethyl formamide (DMF), Polyvinylidene difluoride (Sigma Aldrich), surfactant Span-80 and as synthesized GFO nano-powder. Initially, GFO nanopowder (10 wt.%, 20 wt.%, 30 wt. % with respect to PVDF) was mixed with ethanol and water for 1 h to achieve OH order in the surface of GFO nanopowder.[6] The mixture was then dried at 80° C. Surfactant Span-80 and solvent acetone was added to the above and stirred overnight. After removal of acetone 8 wt. % PVDF dissolved in DMF was mixed with the above GFO nano-powders. The solution was then poured into a petri dish and heated at 100° C to remove all residual solvent present in it.

### 2.3 Characterization

To perform the structural characterization of the samples, x-ray diffraction of synthesized nanopowders and polymeric composites were performed using Rigaku diffractometer with CuK $\alpha$  radiation. Morphological evolution of GFO/PVDF composites was examined by scanning electron microscopy (SEM). Room temperature Fourier transform infrared spectra (FTIR) were also studied. The output voltage and the current generated by the composites were measured by using a Kiethley 6517B electrometer.

## 3. Results and Discussion

### 3.1 X-ray diffraction analysis

Fig. 1 shows the XRD patterns of PVDF and GFO-PVDF composites synthesized with various weight fractions of GFO. PVDF exists in three crystalline phases (i.e.  $\alpha$ ,  $\beta$ ,  $\gamma$ - phase). There are two intense peaks observed at  $2\theta \sim 17.7^\circ$ ,  $19.9^\circ$  and  $26^\circ$  assigned to  $\alpha$ -phase.[7-9] The peak position corresponding to  $35.6^\circ$  and  $38.3^\circ$  could be indexed to  $\beta$ - phase and  $\alpha$ -phase of PVDF, respectively.[8] The XRD pattern of GFO nanopowder over  $2\theta \sim 20^\circ - 80^\circ$  indexed with JCPDS card no. 76-1005 is shown in the inset of Fig. 1. From the figure, orthorhombic  $Pc2_1n$  symmetry of GFO is evident without presence of any secondary phase. Fig. 1 shows that with increase in GFO concentrations in PVDF matrix, the

diffraction peak intensities of PVDF gradually decrease and the peaks of GFO became prominent. It is also clear that, the nature and positions of GFO peak remain almost unaltered with change in GFO weight percent. So we conclude that structure of GFO remains un-affected upon blending with PVDF matrix.

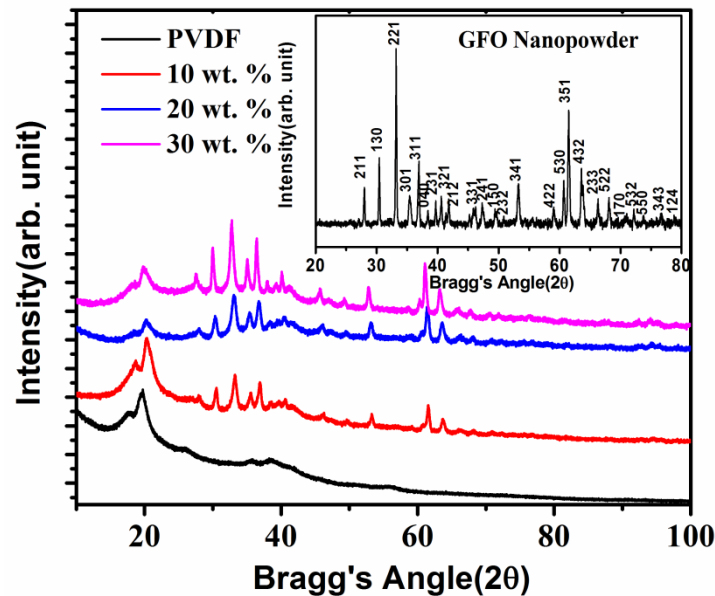


Fig. 1 Room temperature x-ray diffraction patterns of PVDF and GFO-PVDF nano-composite films with various weight percentage of GFO. Inset shows XRD pattern of GFO nano-powder indexed with JCPDS card no. 76-1005.

### 3.2 Microstructural analysis

The microstructures of the samples were examined by scanning electron microscopy (SEM). The SEM micrographs of pure PVDF, 10-30 wt. % GFO-PVDF composites are shown in Fig. 2(a-d), respectively. From Fig. 2(a), it was seen that pure PVDF film is clean, neat and uniform without any pores but it changes as the concentration of GFO nanoparticles changes in the polymer matrix. The micrographs reveal the uniform distribution of GFO nanopowders in the PVDF polymer matrix with no pores. In 10 wt. % of GFO-PVDF composite grains can be seen. As the concentration of GFO increases, packing of particles became denser. So we can say that there is excellent compatibility between PVDF and GFO nanoparticles. Inset of Fig. 2(d) shows the optical image of the 30 wt. % GFO-PVDF composite film and it was found that the composite film was quite flexible.

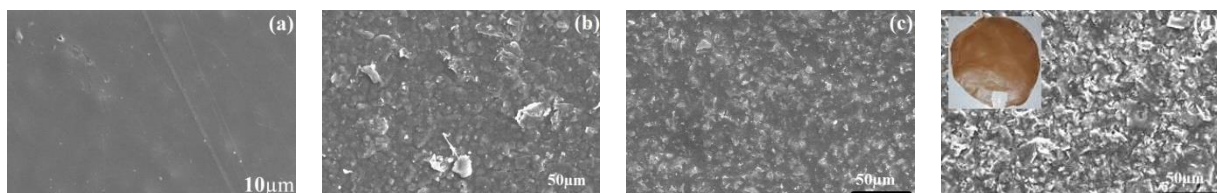


Fig. 2 (a) SEM image of pure PVDF. (b-d) SEM images of 10-30 wt. % of GFO-PVDF composite films, respectively. Inset of Fig. 2(d) shows optical image of 30 wt. % GFO-PVDF composite film.

### 3.3 FTIR analysis

Phase evolution of GFO-PVDF nanocomposite was further studied using FTIR analysis. Fig. 3 plots the FTIR spectra of pure PVDF and GFO-PVDF composites with different weight percentages of GFO in the spectral range of 650-2000  $\text{cm}^{-1}$ . As discussed earlier, PVDF exists in  $\alpha$ ,  $\beta$ ,  $\gamma$  phases. Bands at 759 ( $\text{CH}_2$  stretching) and 971  $\text{cm}^{-1}$  are related to  $\alpha$ -phase. The  $\beta$  phase is observed at 833, 871, 1169 and 1279  $\text{cm}^{-1}$ . [6] The 680  $\text{cm}^{-1}$  band is due to head to head and tail to tail arrangements. The band at 833  $\text{cm}^{-1}$  is due to  $\text{CH}_2$  rocking,  $\text{CF}_2$  stretching, skeletal C-C structure and stretching in  $\beta/\gamma$  phase. The band at 1067  $\text{cm}^{-1}$  is assigned to  $\text{CH}_2$  wagging. Similarly, the band at 1169  $\text{cm}^{-1}$  is assigned to symmetrical stretching of  $\text{CF}_2$  groups and  $\beta$  - phase, 1279  $\text{cm}^{-1}$  is assigned to  $\text{CF}_2$  symmetric stretching and  $\beta$ - phase, 1405  $\text{cm}^{-1}$  is marked to  $\text{CF}_2$  symmetric stretching and  $\alpha$ - phase. [8] Most of the vibrational bands of  $\beta$  and  $\gamma$  phases appear at the same frequencies due to the presence of tail to tail structure in the chain configuration of PVDF. [10] The  $\alpha$ - phase becomes quite weak with gradual increase in GFO concentration. Most of the PVDF peaks are present in FTIR spectra. A few vibrational frequencies below 800  $\text{cm}^{-1}$  disappeared which suggests interaction between PVDF and GFO during formation of PVDF-GFO nano-composite. PVDF's original structure is changed and some groups in PVDF are fixed in GFO. As the concentration of GFO increases, some vibrational bands of PVDF gradually decreases. [11]

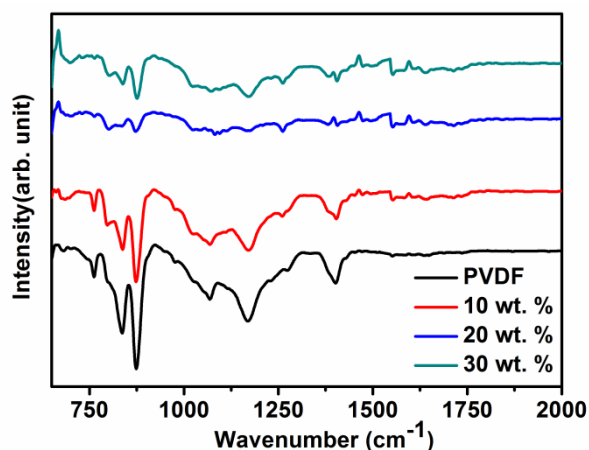


Fig. 3 FTIR spectra of GFO-PVDF nanocomposites and PVDF.

### 3.4 Electrical characterization

The above synthesized nano GFO-PVDF free standing flexible composite films were subjected to energy harvesting studies. The composite films were cut into  $1.5 \times 1.5 \text{ cm}^2$  dimension and silver paste was applied on both the sides of the films to act as electrodes. Two thin connecting wires were placed on both sides of the film and the whole system was laminated to make the final device. Fig. 4 shows a representative image of the final device. The output voltage and current were measured by manually finger tapping on the device. Fig. 5(a-c) shows the output voltage generated by 10-30 wt. % composite films. The 10 wt. % GFO-PVDF composite generates an output voltage of 1.5 V (Fig. 5(a)). With increasing GFO content the output voltage increased to 3 V and 4 V, respectively for 20 and 30 wt. % of GFO. Fig. 5(d-f) shows the output current generated by 10-30 wt% GFO-PVDF composite films. Fig. 5(d) shows that 10 wt. % composite film generates an output current of  $1.2 \times 10^{-11}$  Amp. With increase in GFO content in polymer matrix the output current increased to  $6 \times 10^{-10}$  Amp for 20 wt. % and  $4 \times 10^{-9}$  Amp for 30 wt. % of GFO.

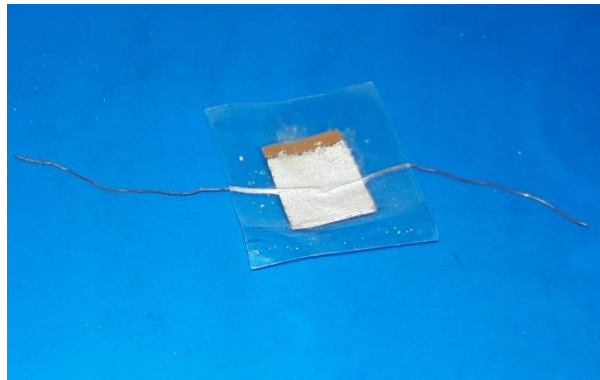


Fig. 4 Optical image of flexible composite device with 30 wt. % of GFO.

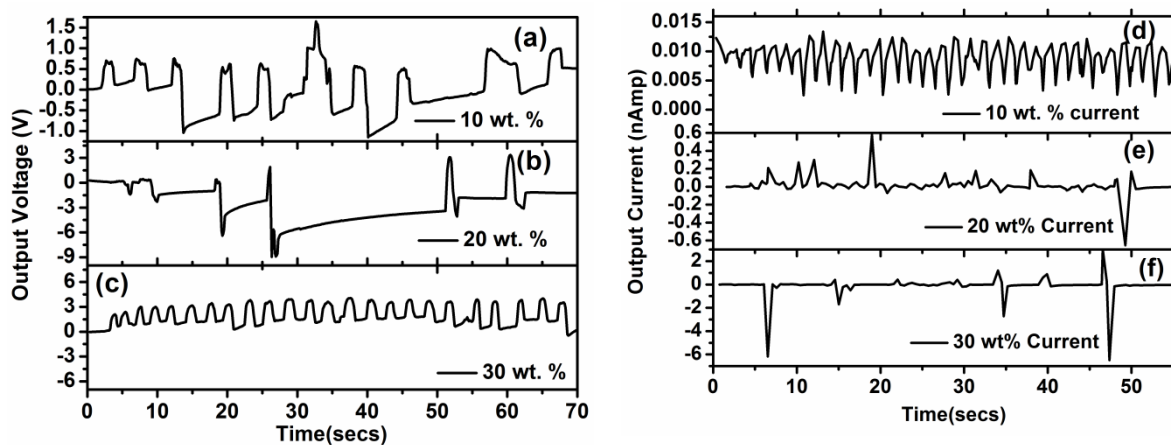


Fig. 5 Output voltage signal of (a) 10 wt. %, (b) 20 wt. %, (c) 30 wt. % GFO-PVDF composite films, respectively. Output current signal of (d) 10 wt. %, (e) 20 wt. %, (f) 30 wt.% GFO-PVDF composite films, respectively.

The voltage generated with increasing GFO content is at par the PVDF based energy harvesting devices.[3, 12] However, the current output of our films is low compared to recent reports on PVDF based nano-composite energy harvesters.[3, 12] The output current could be improved by modifying the composite materials. Multi-walled carbon nanotubes (CNT), reduced graphene oxide (RGO) could be incorporated as conductive fillers to improve the current output.[13, 14]

#### 4. Conclusion

Using solvent casting method thick films of GFO-PVDF composites are produced. XRD and FTIR analysis confirms the presence of  $\alpha$ ,  $\beta$ ,  $\gamma$  phase in PVDF. SEM reveals the uniform structure of PVDF with no pores and the uniform dispersion of GFO in polymer matrix. The investigation on output voltage and current reveals that 30 wt. % GFO-PVDF composite film shows maximum voltage of 4 V and maximum current of 4 nA, respectively. This output voltage is comparable with other reported flexible piezoelectric composites. The output current characteristics could be improved by modifying the synthesis of composite material. Hence, flexible nano GFO-PVDF composites could be a promising candidate for piezoelectric energy harvesting.

### Acknowledgement:

Authors acknowledge support from grant no. IFA-13/MS-03 by Department of Science and Technology, India under INSPIRE faculty award program with. A. Roy acknowledges financial support from SERB, Govt. of India through project no. YSS/2014/000287.

### References

1. Li, H., C. Tian, and Z.D. Deng, *Energy harvesting from low frequency applications using piezoelectric materials*. Applied Physics Reviews, 2014. 1(4): p. 041301.
2. Nunes-Pereira, J., et al., *Energy harvesting performance of piezoelectric electrospun polymer fibers and polymer/ceramic composites*. Sensors and Actuators A: Physical, 2013. 196(Supplement C): p. 55-62.
3. Nunes-Pereira, J., et al., *Energy harvesting performance of BaTiO<sub>3</sub>/poly(vinylidene fluoride–trifluoroethylene) spin coated nanocomposites*. Composites Part B: Engineering, 2015. 72(Supplement C): p. 130-136.
4. Remeika, J.P., *GaFeO<sub>3</sub>: A Ferromagnetic-Piezoelectric Compound*. Journal of Applied Physics, 1960. 31(5): p. S263-S264.
5. Kavita, S., et al., *Magnetic and 57 Fe Mössbauer study of magneto-electric GaFeO<sub>3</sub> prepared by the sol–gel route*. Journal of Physics: Condensed Matter, 2013. 25(7): p. 076002.
6. Luo, B., et al., *Fabrication, characterization, properties and theoretical analysis of ceramic/PVDF composite flexible films with high dielectric constant and low dielectric loss*. Journal of Materials Chemistry A, 2014. 2(2): p. 510-519.
7. Sita, M.D., et al., *Structural changes in PVDF fibers due to electrospinning and its effect on biological function*. Biomedical Materials, 2013. 8(4): p. 045007.
8. Dash, S., R.N.P. Choudhary, and M.N. Goswami, *Enhanced dielectric and ferroelectric properties of PVDF-BiFeO<sub>3</sub> composites in 0–3 connectivity*. Journal of Alloys and Compounds, 2017. 715: p. 29-36.
9. Tan, K.S., et al., *Pyroelectricity enhancement of PVDF nanocomposite thin films doped with ZnO nanoparticles*. Smart Materials and Structures, 2014. 23(12): p. 125006.
10. Mandal, D., K. Henkel, and D. Schmeißer, *The electroactive β-phase formation in Poly(vinylidene fluoride) by gold nanoparticles doping*. Materials Letters, 2012. 73: p. 123-125.
11. Yang, C., H.-s. Song, and D.-b. Liu, *Effect of coupling agents on the dielectric properties of CaCu<sub>3</sub>Ti<sub>4</sub>O<sub>12</sub>/PVDF composites*. Composites Part B: Engineering, 2013. 50: p. 180-186.
12. Karan, S.K., D. Mandal, and B.B. Khatua, *Self-powered flexible Fe-doped RGO/PVDF nanocomposite: an excellent material for a piezoelectric energy harvester*. Nanoscale, 2015. 7(24): p. 10655-10666.
13. Bhavanasi, V., et al., *Enhanced Piezoelectric Energy Harvesting Performance of Flexible PVDF-TrFE Bilayer Films with Graphene Oxide*. ACS Applied Materials & Interfaces, 2016. 8(1): p. 521-529.
14. Das, S., et al., *Electrical and mechanical behavior of PMN-PT/CNT based polymer composite film for energy harvesting*. Applied Surface Science, 2018. 428(Supplement C): p. 356-363.